Microelectronics Reliability 52 (2012) 1753–1760

Contents lists available at SciVerse ScienceDirect

Microelectronics Reliability

journal homepage: www.elsevier.com/locate/microrel

Time dependent dielectric breakdown physics – Models revisited

J.W. McPherson *

McPherson Reliability Consulting LLC, 2805 Shelton Way, Plano, TX 75093, USA

ARTICLE INFO

Article history:
Received 26 May 2012
Accepted 6 June 2012
Available online 4 July 2012

ABSTRACT

Time-Dependent Dielectric Breakdown (TDDB) models for silica(SiO_2)-based dielectrics are revisited so as to better understand the ability of each model to explain quantitatively the generally accepted TDDB observations. Molecular dielectric degradation models, which lead to percolation path generation and eventual TDDB failure, tend to fall into three broad categories: field-based models, current-based models, and complementary combinations of field and current-based models. A complementary combination of field-induced polar-bond stretching and current-induced bond-catalysis seems to be required, at the molecular level, to explain the generally accepted TDDB observations. Thus, TDDB modeling is not simply the use of field or current – but both. Complementary combinations of field and current are required to fully explain the generally accepted TDDB observations.

1. Introduction

Time-Dependent Dielectric Breakdown (TDDB) refers to the physical process whereby a dielectric stored under a constant electric field, less than the materials breakdown strength, will break down with time. Breakdown is a term used to describe the dielectric phase transition from insulating phase to a more conductive phase.

Time-Dependent Dielectric Breakdown (TDDB) in silica(SiO_2)-based dielectrics is one of the more important failure mechanisms for Integrated Circuits (ICs) because ICs make extensive use of metal-oxide-silicon field effect transistors (MOSFETs). For this reason, TDDB is also one of the more studied IC failure mechanisms [1–20]. However, a comprehensive molecular-model for TDDB is still somewhat speculative. Physics-based models for TDDB include: field-based models [1–20], current-based models [21–24], or a combination of field and current-based models [25,13]. A combination of field and current-based models seems to be needed because a purely field-based model or a purely current-based model cannot explain quantitatively all the TDDB observations.

In this paper the TDDB focus will be on silica (SiO_2) with the understanding that we are discussing *intrinsic* TDDB properties of silica. By intrinsic it is meant that the silica material is free of unwanted impurities, such as Na^+ (or other metal ions), which can have a dramatic effect on silica TDDB behavior. Thus, our focus will be on how intrinsic molecular Si—O bonds can be distorted/broken by field and/or current to generate the neutral-defects/broken-bonds which are thought to be the precursors of TDDB.

While general/wide-spread acceptance of a single TDDB model for intrinsic silica may be lacking, there are certain TDDB observations for intrinsic silica that do have wide-spread acceptance:

- TDDB is strongly field dependent.
- TDDB can be strongly temperature dependent.
- Activation energy can be field dependent.
- TDDB can be polarity dependent.
- Field acceleration parameter increases with dielectric constant *k*.
- Irreversible neutral-traps/defects/broken-bonds are generated during TDDB stressing.
- Electron spin resonance (ESR) signal increases during TDDB stressing.
- Generation of the defects/broken-bonds leads to a conductive percolation-path formation that eventually triggers breakdown.
- Statistics of TDDB can be described by the Weibull distribution (consistent with Poisson area scaling).
- Polar dielectrics (polar-bonded dielectrics) such as silica show TDDB behavior while non-polar(covalent-bonded) dielectrics generally do not.

The most widely used TDDB models are revisited so as to reevaluate each model relative to its ability to explain quantitatively, at the molecular level, the generally accepted TDDB observations listed above.

2. Molecular bonding in silica

In amorphous silica, [26] each Si-ion is bonded to four neighboring O-ions in a tetrahedral arrangement (O—Si≡O_3) as illustrated

* Tel.: +1 972 955 9617.
E-mail address: mcpherson.reliability@yahoo.com

0026-2714/$ - see front matter © 2012 Elsevier Ltd. All rights reserved.
http://dx.doi.org/10.1016/j.microrel.2012.06.007

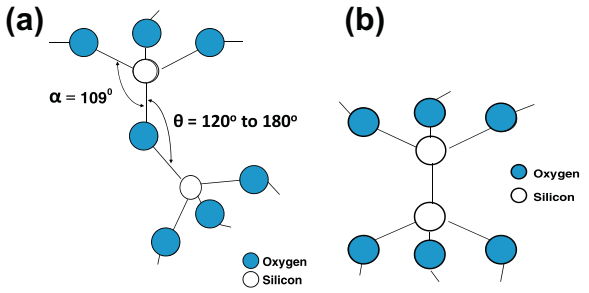

Fig. 1. (a) Si—ion is fourfold coordinated in a tetrahedral configuration with rigid bonding angle $\alpha = 109°$. Each O—ion is twofold coordinated with flexible $\theta = 120–180°$ bonding angles. (b) Oxygen vacancy leads to weak Si—Si bonding.

in Fig. 1a. In this configuration, the Si-ion is said to have a coordination number of $CN = 4$. Due to sp^3 hybridization, the bonding of the Si-ion to its neighboring O—ions is strongly directionally dependent, i.e., the O-Si-O bonding angle α is relatively rigid at $\alpha = 109°$. However, the Si—O—Si bonding angle θ is relatively flexible and bonding can occur in a fairly wide range of angles: $\theta = 120–180°$. It is the flexibility of the Si—O—Si bonds (θ flexibility) that permits nearly all bonds in silica to be satisfied even in an amorphous network. In the work which follows, it will be very important to remember that for a neutral bond, there are two electrons in the bond with opposite spins.

If the silica growth/deposition conditions are such that all bonds cannot be satisfied in the amorphous network, then naturally occurring intrinsic molecular defects (such as oxygen vacancies or silicon vacancies) can form leading to relatively weak Si—Si bonding ($O_3{\equiv}Si—Si{\equiv}O_3$) [as illustrated in Fig. 1b] or an even weaker O—O bonding ($O_3{\equiv}Si—O—O—Si{\equiv}O_3$).

The Linus Pauling approach [27] to chemical bonding will be used in this paper so as to obtain a more fundamental understanding of the Si—O bond strength and bond polarity. The bond energy ϕ for the elemental Si—Si bonding and O—O bonding have been determined from mean-bond enthalpy measurements and found to be: $\phi_{Si-Si} = 1.8$ eV and $\phi_{O-O} = 1.4$ eV [28].

The Si—O bond is a very interesting chemical bond because the covalent and polar components of the bond are similar in magnitude. Again, following Pauling's approach for describing the Si—O bond, one can estimate the covalent and polar components of the bonding energy as:

$$(\phi_{si-o})_{covalent} = \sqrt{\phi_{si-si} \bullet \phi_{o-o}} \cong 1.6\ eV \tag{1}$$

and

$$(\phi_{si-o})_{polar} = 1.3(X_o - X_{si})^2 eV \cong 3.8\ eV \tag{2}$$

where X_{Si} and X_O represent the electronegativities of silicon (1.8) and oxygen (3.5), respectively.

A mean Si—O bond strength of 5.4 eV is consistent with experimental evidence and molecular bond calculations [29–34]. Since the Si-ion is fourfold coordinated, then its total bond energy is approximately 21.6 eV whereas an O-ion is twofold bonded giving its total bond energy to be approximately 10.8 eV. Since bonding energies are negative, one can understand (from a lower free energy perspective) that it is much more likely for oxygen vacancies to occur naturally in silica versus silicon vacancies. The primary intrinsic defect in silica that could be impacting TDDB is the oxygen vacancy ($O_3{\equiv}Si—Si{\equiv}O_3$).

Polar nature of molecular bonds in dielectric materials is emphasized in this paper because non-polar bonded (covalent-bonded) dielectrics do not undergo TDDB.

While covalent-bonded dielectrics do have a critical current density J_{crit} at which thermal failure can occur (Joule-heating induced failure), they can be stressed at 80–90% of this critical current density for very long periods of time without undergoing TDDB.

Covalent-bonded dielectrics that do not undergo TDDB include: silicon (with a dielectric constant $k = 12$), germanium($k = 6$), and carbon in the diamond structure (diamond: $k = 6$). Because of their relatively small band gaps, normally we think of silicon and germanium as being important semiconductors. However, at low temperatures, silicon is an excellent insulator and for this reason silicon is often used in solid-state radiation detectors. Carbon, in the diamond structure, because of its wide band gap (5.4 eV) is usually thought of as an insulator at nearly all temperatures. As shown in the Table 1, covalent-bonded dielectrics (Ge, Si, C) with tetrahedral coordination do not tend to show TDDB behavior, but important polar-bonded dielectrics such as SiO_2($k = 3.9$) and S_3N_4 ($k = 7.5$) do exhibit TDDB behavior.

Since polar bonding seems to be of intrinsic importance to the discussion of TDDB, a closer investigation of polar-bonding of molecules is warranted. Bond polarity can be described by the fraction f^* of polar bonding energy versus total bonding energy:

$$f^* = \frac{(\phi_{Si-O})_{Polar}}{(\phi_{Si-O})_{Polar} + (\phi_{Si-O})_{Covalent}} = 0.7. \tag{3}$$

3. Bond distortion produced by electric fields

As is illustrated in Fig. 2, when an external electric field E_{ox} is applied to a polar dielectric material of dielectric constant k, a local electric field E_{loc} tends to develop which distorts the polar tetrahedral bonds $O—Si{\equiv}O_3$. The top Si—O bond (Fig. 2b) is severely stretched in a state of tension while the lower bonds $Si{\equiv}O_3$ bonds are compressed. The strained bonds induce a net dipole moment in the direction of the electric field.

The local electric field E_{loc} (Mossotti field) is a sum of the external electric field plus the field contribution from the induced dipole moments and it is generally described by the Lorentz relation (valid for cubic and amorphous materials):

$$E_{loc} = \left(\frac{2+k}{3}\right) E_{ax}. \tag{4}$$

For silica, with a dielectric constant of $k = 3.9$, one can see that the local field E_{loc} (which brings about bond distortion) is roughly twice that of the external field.

Table 1
Comparison of polar and non-polar dielectrics.

Material	Band gap, *Eg* (eV)	Dielectric constant, *k*	Metal–ion coordination	Bonding	TDDB behavior
Germanium	0.66	6	Tetrahedral	Covalent	No
Silicon	1.12	12	Tetrahedral	Covalent	No
C (diamond)	5.4	6	Tetrahedral	Covalent	No
Silicon Dioxide	8.9	3.9	Tetrahedral	Polar	Yes
Silicon Nitride	5.0	7.5	Tetrahedral	Polar	Yes

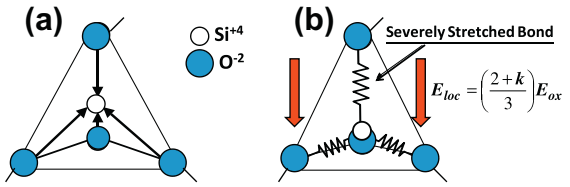

Fig. 2. (a) Normal tetrahedral polar bonding of the Si-ion to the four neighboring O-ions is shown. Arrows indicate the directions of the electric dipole moment for each Si—O bond. (b) Bond-distortion is caused by the local electric field E_{loc}.

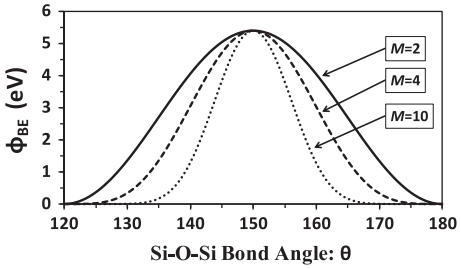

Fig. 4. Bond energy/strength versus Si—O—Si bonding angle θ is shown. Bond's flexibility described by exponent M.

4. Bond-breakage/coordination-breakage

Bond/Coordination breakage is required to produce the increase in ESR signal observed during TDDB testing. These generated defective sites are thought to form the backbone for percolation path [38,39] which triggers TDDB.

4.1. Role of oxygen vacancies in bond breakage

The defects generated during TDDB stressing are believed to be primarily neutral because any flat-band voltage changes, for Metal-Oxide-Silicon (MOS) devices, are typically small during the TDDB stressing. Furthermore, it is thought that these neutral defects must be related to a defect generation process which is molecular in origin. Also, the defect generation process is observed to be irreversible (e.g., if during TDDB stressing, one simply stops the TDDB test mid-term and bakes/anneals the device and then puts the device back on TDDB testing – one sees little evidence of increased TDDB lifetime) [7]. Likewise, if the TDDB testing is interrupted mid-term and the electric field is reversed – one sees little evidence of a strong increase in TDDB lifetime) [8]. Thus, we conclude that the damage to the silica molecular structure during TDDB testing is locked into the lattice and that the damage is approximately irreversible. Irreversible molecular damage in a solid is normally associated with a change in bonding coordination via: atom translation, atom rotation, or both.

Shown in Fig. 3 is an example of a dangling-bond creation/generation from the oxygen vacancy. A dangling bond is created/generated when the bottom silicon ion collapses (under the influence of the local electric field) from the fourfold coordinated sp^3 tetrahedral coordination to the threefold coordinated sp^2 (planar hybridization). This stress relaxation process creates a dangling bond (E' *center*) containing a single electron.

The spin of a single electron will give rise to a magnetic moment which is responsive to an ESR signal [35–37] and thus satisfies one of the important TDDB observations. Whether this Si—Si bond breakage mechanism is irreversible (recovers with field reversal or baking) depends on the amount of lattice relaxation that occurs once the bond is broken. If the local lattice relaxation is significant, then the broken bond will be locked-in and will tend not to recover with either field reversal or with baking, another important TDDB observation.

4.2. Impact of bonding angle on bond breakage

The bond strength depends on the Si—O—Si bonding angle θ and can be approximated by:

$$\phi_{BE}(\theta - \theta_{eq}) = (\phi_{BE})_{eq} cos^{M}[3|\theta - \theta_{eq}|], \tag{5}$$

where $(\phi_{BE})_{eq}$ = 5.4 eV is the equilibrium bond strength at θ_{eq} = 150° and M is the flexibility exponent (M = 2 if the bond angle is relatively flexible while $M > 2$ for relatively inflexible bond angles) as illustrated in Fig. 4.

Shown in Fig. 5a is a strained Si—O—Si bond with $\theta \approx 180°$. A shearing stress produced by the local electric field (Fig. 5b) has little difficulty in breaking such a bond as illustrated in Fig. 5c.

4.3. Coordination breakage versus bond breakage

Since the breakage of Si—O bonds seems to be required for a fundamental understanding intrinsic TDDB behavior in silica, perhaps it very important and instructive to look more closely at the Si—O bonding potential. This has been investigated using a Mie-Grüneisen bonding potential of the form [15]:

$$\phi(r) = \phi_{BE}\left(\frac{mn}{m-n}\right)\left[\frac{1}{m}\left(\frac{r_0}{r}\right)^{m} - \frac{1}{n}\left(\frac{r_0}{r}\right)^{n}\right], \tag{6}$$

where: ϕ_{BE} is the bond energy, m is the repulsive exponent for the bond and n is the attractive exponent for the bond.

ϕ_{BE} is the total energy required to break a bond in tension (to separate the Si-ion and the O-ion by an infinite distance) and is expected to be 5.4 eV. However, in a real solid, the bonded atoms are not displaced to infinity – often the bonded atoms are only displaced a very short distance or undergo a slight rotation. These

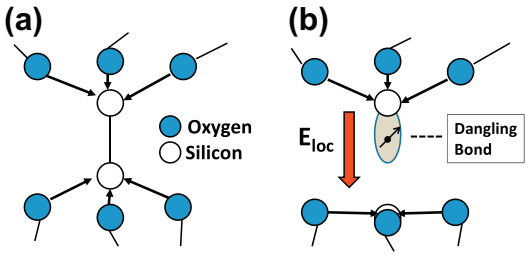

Fig. 3. (a) Naturally occurring oxygen vacancies in silica can result in relatively weak Si—Si bonding. (b) Under the presence of a large local electric field there is a strong driving force for the electric dipole moments (in lower half of molecule) to flip in a direction so as to reduce their dipolar-field energy. This electric-dipole flipping can occur only if the Si—Si bond breaks.

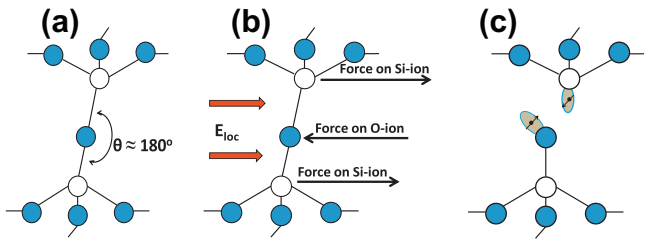

Fig. 5. (a) Strained Si—O—Si bonding illustrated near the bonding limit of $\theta \approx 180°$. (b) A shearing stress, due to the local electric field, can easily break such a bond. (c) The bond-breakage process leaves behind a neutral molecular structure which can be ESR active. Lattice-relaxation/stress-relief ((a) versus (c)) can make the bond-breakage process irreversible.

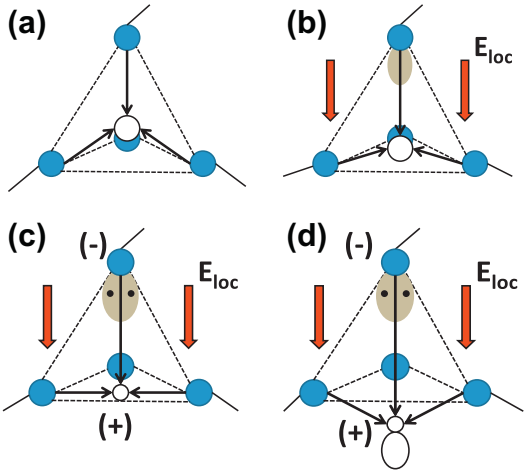

Fig. 6. (a)Normal tetrahedral O—Si═O_3 bonding is shown. (b) Local electric field E_{loc} distorts the bonds putting the top Si—O bond in tension and a shift in the electron cloud more toward the O-ion. (c) Electron is transferred from Si-ion to O-ion, making the Si-ion smaller thus facilitating collapse of the Si-ion into the basal plane. (d) Lowest energy configuration is the so-called *pucker* configuration (slightly beyond the basal plane).

bonding changes can be more accurately described as coordination breakage as opposed to bond breakage. It has been previously shown that coordination breakage processes are possible which require much less energy than 5.4 eV [17]. One such mechanism is illustrated in Fig. 6 where a coordination breaking process (versus bond-breakage process) is shown.

The energy required, for example, to displace the Si-ion from fourfold coordination to threefold coordination [as illustrated in Fig. 6] is less than the normal Si—O bond breakage energy. As the Si-ion moves toward the basal plane it will start to give-up more of its electron cloud to the top Oi-on such that the Si—O bond becomes even more ionic (with a smaller Si ionic-radius) thereby enabling its final collapse into the basal plane. Thus, it is only the covalent part of the Si—O bond which is actually broken by the coordination change from *CN* = 4 to *CN* = 3 because most of the ionic component remains. The energy required to break coordination is significantly lower (~2.4 eV) versus the energy to break the bond (~5.4 eV) [17].

5. Conduction processes in silica

Previous section discussed the impact of field on the molecular bonds. Here we want to understand the conduction process(es) in silica and then we will attempt to see how the conduction process(es) could impact Si—O bond strengths.

In Fig. 7(a), the band structure of silica is shown. Fowler–Nordheim conduction in silica is shown in Fig. 7b. The Fowler–Nordheim (F–N) conduction equation is given by:

$$J_{F-N} = AE_{ox}^2 \exp\left[-\frac{B}{E_{ox}}\right]. \tag{7}$$

One can see from Fig. 7b that, due to barrier height of silica, in order to get significant F–N conduction in silica the electric field in the oxide must be high (>5 MV/cm). Eq. (7) shows no explicit temperature dependence in the F–N conduction equation and this agrees with experiment which finds that the activation energy for F–N conduction in silica is very low (<0.05 eV).

If deep traps exist (Fig. 8a), or are generated in the silica during stressing, then a trap-assisted tunneling current can exist leading to pre Fowler–Nordheim conduction as illustrated in Fig. 8b. If the traps, as illustrated in Fig. 8a are very shallow (only a few tenths eV) then Poole–Frenkel conduction in the dielectric can occur and is generally described by the equation,

$$J_{P-F} = CE_{diel}\left[\frac{-q(\phi_B - \sqrt{qE_{diel}/(\pi\varepsilon)})}{K_B T}\right]. \tag{8}$$

We note that for Poole–Frenkel (P–F) conduction, this conduction mechanism is significant only if the barrier height ϕ_B is a few tenths eV. We also note that the role of the field is to reduce the barrier height and thereby enhance the conduction. Often Poole–Frenkel conduction is used for silica which contains an extensive amount of impurities – such as low-k silica-based dielectrics which have pores often containing carbon clusters [50–53].

6. Frequently used TDDB models

The most frequently used TDDB models are based on field-induced degradation, or current-induced degradation, or a combination of field-induced and current-induced degradation.

6.1. Thermochemical E-Model

In thermochemical theory, the bond/coordination breakage rate constant κ for strained molecules depends on the number of times per sec υ_0 that the strained molecule interacts with the surrounding lattice (υ_0 = vibration frequency ≈10^{13}/s) times the Boltzmann probability that, on a given interaction with the lattice, the bond will receive enough energy to break the bond/coordination [4–20]. Thus, bond breakage is a phonon driven process and the rate constant κ for breakage is given by:

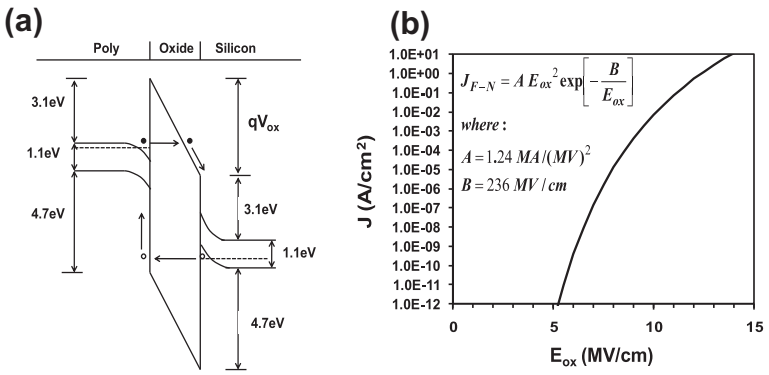

Fig. 7. (a) Band Structure for silica. (b) Typical Fowler–Nordheim conduction is silica.

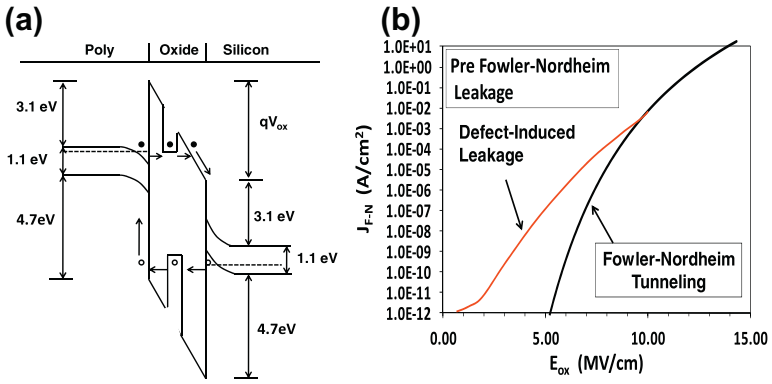

Fig. 8. (a) Deep traps illustrated in silica. (b) Trap assisted tunneling can foster a Pre Fowler–Nordheim conduction/leakage.

$$\kappa = \upsilon_0 \exp\left[-\frac{\Delta H}{K_B T}\right]. \tag{9}$$

ΔH is the enthalpy of activation (usually referred to simply as activation energy) and represents the energy required to break the bond/coordination. However, since the external field serves to distort/weaken the bonds, the energy required to activate bond/coordination breakage reduces with external field is given by the relation [15]:

$$\Delta H = \Delta H_0 - p_{eff}(m,n)E_{ox}, \tag{10}$$

where ΔH_0 is the energy required to break the bond/coordination in the absence of external electric field. $p_{eff}(m\ n)$ is the effective dipole moment for bond/coordination breakage process and is given by:

$$p_{\text{eff}}(m,n) = (z^* e) r_0 [\eta(m,n)]^{-1} \left(\frac{2+k}{3}\right), \tag{11}$$

where z^* is the number of electron charges on the Si^{+4} ion ($z^* = 4f^*$), r_0 is the equilibrium Si—O bond distance (1.7 Å), η depends only on the bonding exponents (the values for η are given in the Appendix), and k is the dielectric constant for silica ($k = 3.9$). For Born-Landé ionic-type bonding ($m = 9, n = 1$) we obtain $p_{\text{eff}}(9\,1) = 13.3$ eÅ. If the bonding starts to take on more of a covalent component, we obtain $p_{\text{eff}}(9\ 2) = 7.5$ eÅ. Is is important to stop here and recognize that if the molecular bond has no dipole moment, then TDDB is not expected. This *E*-model prediction matches an important TDDB observation – non-polar dielectrics (covalent-bonded dielectrics) do not undergo TDDB.

The time-to-failure is assumed to be inversely proportional to the bond/coordination breakage-rate constant κ:

$$TF = A_0 \exp\left[\frac{\Delta H_0}{K_B T} - \gamma E\right], \tag{12}$$

where

$$\gamma = -\left[\frac{\partial \ln(TF)}{\partial E}\right]_{T=constant} = \frac{P_{\text{eff}}}{K_B T}. \tag{13}$$

γ is referred to as the field acceleration parameter. Thus, the thermochemical *E*-Model gives a quantitative estimate of the activation energy ΔH [Eq. (10)] and the field acceleration parameter γ [Eq. (13)] with p_{eff} predicted to be in the range of 7–14 eÅ. Also, Eqs. (11) and (13) show that the field acceleration parameter γ increases with dielectric constant, another important TDDB observation [14].

The main criticism of the *E*-Model is that it does not explain polarity dependence (TDDB differences can occur if the roles of anode and cathode are reversed) – a generally accepted TDDB observation. Because of the polarity-dependence deficiency of the *E*-Model, current-based models (which can be polarity dependent) and have gained favor, even though they have their own set of deficiencies.

6.2. 1/E Model (anode hole injection model)

The $1/E$ model was the first current-based TDDB model to gain popularity [21–24]. It is easy to accept the fact that current can produce degradation – if we simply ramp the current through any material (conductor or insulator) it will reach a critical breakdown current J_{crit} at which the device will fail catastrophically (due to excessive Joule-heating effects). In the $1/E$ model for TDDB (even at low fields) damage is assumed to be due to current flow through the dielectric due to Fowler–Nordheim (F–N) conduction. Electrons, which are F–N injected from the cathode into the conduction band of SiO_2, are accelerated toward the anode. Due to impact ionization, as the electrons are accelerated through the dielectric, some damage to the dielectric might be expected. Also, when these accelerated electrons finally reach the anode, holes can be produced which may tunnel back into the dielectric causing damage. This is the anode hole injection (AHI) model and it is illustrated in Fig 9.

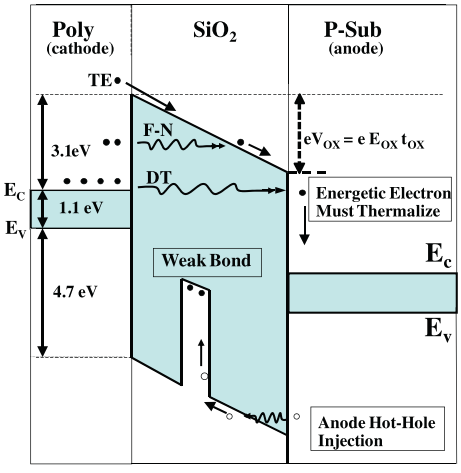

Fig. 9. Very few electrons will have sufficient thermal energy to be thermally emitted (TE) over the barrier. More probable, under high fields, the electrons will Fowler–Nordheim (F–N) tunnel through the barrier. Any electrons reaching the anode will have to thermalize (release their excess energy), occasionally creating an energetic hole which can tunnel back into the gate oxide. A weak bond (a bond with lower bond-strength) will serve as a hole trap. This is the basis for the anode hole injection (AHI) $1/E$ - Model. If the oxide layer is very thin (<5.0 nm), then direct tunneling (DT) is also possible.

Since the electrons (from the cathode) and the injected holes (from the anode) are the result of F–N tunneling conduction, then the time-to-failure is expected to show an exponential dependence on the reciprocal of the electric field, $1/E$:

$$TF = \tau_o(T) Exp\left[\frac{G(T)}{E_{ox}}\right]. \quad (14)$$

In the above TF equation, $G = B + H$, where B is associated with the electron tunneling ($B \sim 240$ MV/cm), and H is associated with the hole tunneling ($H \sim 55$–115 MV/cm), and $\tau_o(T)$ is a temperature dependent pre-factor. Historically, because the $1/E$ model is a conduction model, Q_{bd} (total charge fluence to breakdown) became an often used reliability metric. However, the usefulness of Q_{bd} as an important reliability metric diminished when film thickness became <5.0 nm because of the intrinsic leakiness of hyper-thin silica films.

The main criticism of the $1/E$ Model (AHI theory) is two fold: (1) the hole generation rate at the anode is extremely small at low fields/voltages and (2) the efficiency for the injected holes to produce defects in the silica seems to be very low [54–56] – intended confirmation experiments whereby holes were injected into the oxide via substrate hot-hole injection (SHH) have shown little/no impact on TDDB. In addition, since F–N tunneling is very weakly temperature dependent, no quantitative explanation exists in the present AHI theory to explain the strong temperature dependence observed during TDDB testing.

6.3. Power-law voltage V^N-Model

The power-law V^N-Model [19,40–45] is also referred to as the anode hydrogen release (AHR) model. Si—H bonds at the Si/SiO_2 anode interface are believed to be excited by single-event electron processes (coherent processes) or multi-event electron processes (incoherent processes).

This excitation-process, at the anode is shown in Fig. 10, is thought to lead to hydrogen (or hydrogen-ions) being released into the bulk of the silica. The interaction of this released hydrogen with weak bonds in the bulk is postulated to lead to defective bond generation, percolation path formation, and then eventually TDDB.

The AHR model was originally proposed for hyper-thin dielectrics where ballistic transport dominates. Thus, if the gate voltage is V, then the energy delivered to the anode by each electron is simply $(e) \times (V)$. For silica dielectrics, which are hyper-thin SiO_2 (<40 Å), a power-law voltage model has been proposed for TDDB of the form:

$$TF = B_o(T)[V]^{-N}. \quad (15)$$

For hyper-thin oxide films, the observed exponent is generally in the range: $N = 40$–48. Even though the AHR model was developed under the hyper-thin oxide assumption, sometimes it is applied to thicker films where the justification is less than clear.

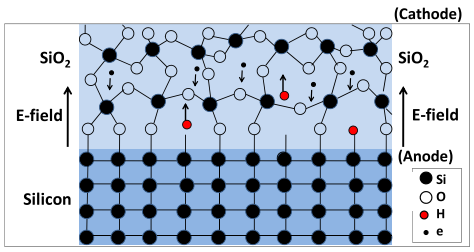

Fig. 10. In AHR Model, hydrogen bonds are thought to be broken by single-event electron processes (coherent processes) or multi-event electron processes (incoherent processes). Released hydrogen atoms(or ions) may diffuse(drift) into the bulk of the silica whereby they are postulated to create damage.

The primary weakness(es) of the AHR model – the theory makes no effort to quantitatively explain the *strong temperature dependence* (high activation energy) associated with TDDB and as to why the activation energy reduces with field.

In addition, the AHR suffers from the *dilution problem*. While the amount of hydrogen at the anode Si/SiO_2 interface might be sufficient to cause TDDB in hyper-thin Si/SiO_2 films, the impact the released hydrogen at the anode must surely be diluted as the thickness of the silica film increases. However, very thick silica films continue to show TDDB behavior [57].

Finally, there are two electrons in the neutral Si—H bond (leading to a bond energy of ~3 eV) and it is unclear as to what exactly happens to these two electrons in AHR theory. The two electrons cannot be excited to the conduction band in SiO_2, at low voltages, because the bandgap is 8.9 eV – so into what available states/bonds do these two electrons reside without violating the *Pauli exclusion principle*?

6.4. Exponential $E^{1/2}$-Model

Exponential $E^{1/2}$ - Model TDDB development [46–49] has been considered for low-k silica-based interconnect dielectrics [50–53]. Current-induced dielectric degradation and TF models assume that the degradation is due to current flow through the dielectric. For high quality SiO_2, the dominant current flow is nearly always Fowler–Nordheim conduction and thus the damage is assumed to follow a $1/E$ Model. However, for other dielectric types, or even poor quality silica dielectrics (such as low-k interconnect dielectrics), the conduction mechanism may be Poole–Frenkel or Schottky conduction. Thus, based on a current-induced degradation, one might expect a TF model of the form for low-k dielectrics:

$$TF = D\ exp\left[\frac{Q_{bh} - \lambda\sqrt{E}}{K_B T}\right]. \quad (16)$$

λ is referred to as the root-field acceleration parameter. As with all the current based models, the primary weakness of the $E^{1/2}$ model – it has great difficulty explaining, quantitatively, the strong temperature dependence (high activation energy) associated with TDDB and as to why the activation energy reduces strongly with field. Recall in P-F conduction, the barrier height Q_{bh} is usually only a few tenths eV while the bond breakage energy is a few eV.

7. TDDB Model comparisons

In Table 2 the generally agreed to TDDB observations are matched with the ability of each model (in its present state of development) to explain the observation. A check mark (✓) is used if the observation is consistent with quantitative model predictions and a question mark (?) is used if the model, in its present state of development, cannot give a quantitative explanation for the observation.

If we compare the models in their present state of development, one might claim that an E-Model plus one of the current based models are perhaps needed to describe quantitatively all the generally agreed to TDDB observations.

8. Which TDDB Model to use?

Since the physics of each of the TDDB models is quite different, then it is only natural to ask the question – *which model should one use?* That is a difficult a question to try to answer, because there seems to be no universal agreement (the physical arguments for each model seem to be reasonable). However, one can certainly ask the question – *what is the relative ranking of the models in terms*

Table 2
TDDB observations versus model predictions.

TDDB observations	*E* Model	1/*E* Model	V^N Model	$(E)^{1/2}$ Model	*E*-Model plus current
Strong field dependence	✓	✓	?	✓	✓
Strong temp dependence	✓	?	?	?	✓
Activation energy reduces with field	✓	?	?	?	✓
Polarity dependent	?	✓	✓	✓	✓
Acceleration increases with dielectric constant	✓	?	?	?	✓
No TDDB for non-polar dielectrics (infinite Qbd)	✓	?	?	?	✓
Degradation continuous and irreversible	✓	✓	✓	✓	✓
Degradation is ESR active	✓	✓	✓	✓	✓
Weibull statistics	✓	✓	✓	✓	✓
Percolation theory	✓	✓	✓	✓	✓

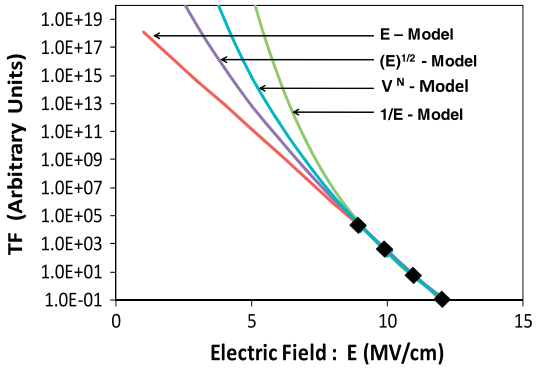

Fig. 11. Shown is the best-fit for each model to the same set of accelerated TDDB data. The *E*-Model gives the shortest time-to-failure when the results are extrapolated to lower electric fields. The 1/*E* Model gives the longest time-to-failure at lower electric fields. One could describe the *E*-Model as being the most conservative and the 1/*E*-Model as being the most optimistic.

of their conservatism? This question does have an easy answer and it is illustrated in Fig. 11. When the models are used to fit to the same set of accelerated TDDB data, the *E*-Model gives a shorter time-to-failure TF, as one extrapolates from high-field accelerated TDDB conditions to lower-field use conditions. This makes the *E*-Model the more conservative model. In terms of relative rank of conservatism: *E*-Model is the most conservative followed by $\sqrt{E}$ -Model, then the power-law *V*-Model and finally the 1/*E* -Model. Thus, the *E* and 1/*E* models tend to serve as *physical guardrails/boundaries* with the other TDDB models fitting in between.

9. Complementary field and current-based TDDB Models

It now seems to be apparent that perhaps one should not think of TDDB just in terms of either a field-based model or a current-based model – but both. The field serves to strain the Si—O bonds (thus weakening the bonds). These weakened bonds can be further excited/catalyzed either by interactions with current-induced electrons, holes or hydrogen ions. This would serve to give a purely field-based model the needed polarity dependence which seems to be missing from the *E*-Model.

As illustrated in Fig. 12, only phonon driven processes have both enough energy and momentum to permanently displace either the Si ion or the O ion and to thus break the strained Si—O bond. However, current-induced interactions with the strained Si—O bond (via current-induced collisions with electrons, holes, or H+ions) can serve to catalyzed the bond breakage process (lower the activation energy for bond breakage).

A complementary approach [25,13] to bond breakage which utilizes both field-induced and current-induced degradation is illustrated in Fig 13. The dual degradation paths are in parallel. The lower path is simply the field-enhanced thermal bond breakage rate constant κ_1 used for the *E*-model. Upper path is the hole-catalyzed field-enhanced thermal bond breakage rate constant κ_2 (driven by 1/E Model). Since κ_2 path is a serial multi-step process, the slowest step (κ_{2a} or κ_{2b} or κ_{2c}) will dominate the degradation rate along this path.

For these parallel complementary degradation paths, the total degradation rate constant is $\kappa_{\text{eff}} = \kappa_1 + \kappa_2$. Since the time-to-failure is inversely proportional to the bond/coordination breakage rate constant κ_{eff}, then one can write [20]:

$$TF = \frac{(TF)_{E-Model}(TF)_{1/E\text{-}Model}}{(TF)_{E-Model} + (TF)_{1/E\text{-}Model}}, \tag{17}$$

where $(TF)_{E\text{-Model}}$ would be the time-to-failure if only degradation path κ_1 was active and $(TF)_{1/E\text{-Model}}$ would be the time-to-failure if only degradation path κ_2 was active. In Fig. 14 this complementary approach was used to fit the TDDB data over a very wide range of field.

While this complementary approach was used for combining the *E*-Model and 1/*E*-Model physics, one could also use this complementary approach to combine any combination of the models.

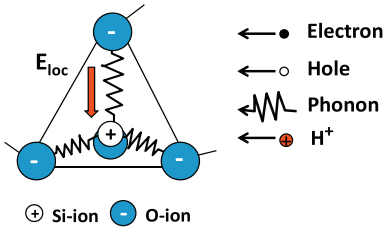

Fig. 12. Several important interaction mechanisms are illustrated for the strained Si—O bond.

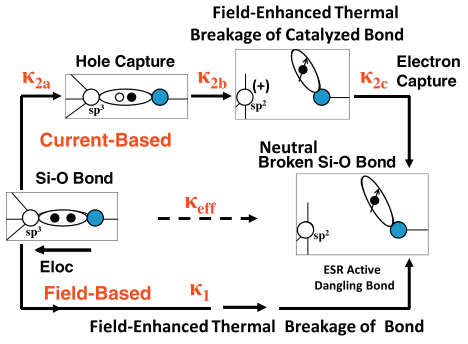

Fig. 13. Complementary field-induced and current-induced degradation paths are illustrated. Lower degradation path is simply the *E*-Model bond-breakage process. Upper degradation path is the hole-catalyzed (AHI Model) bond-breakage process.

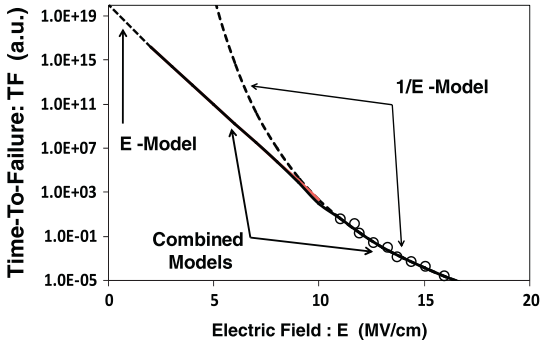

Fig. 14. Complementary approach to incorporating both field-based and current-based models. 1/*E* model fitting of TDDB data above 10 MV/cm and *E*-Model fitting below 10 MV/cm.

This method eliminates the severe restriction of having to choose between extremes: either the most conservative model (*E*-model) or the most optimistic model (1/*E* Model). This complementary modeling approach thus serves as a practical reliability engineering solution to TDDB model use.

10. Conclusions

At the present stage of TDDB model development, neither a purely field-based TDDB model nor a purely current-based TDDB model can explain quantitatively all the generally accepted TDDB observations. Due to polar bonding in silica, the local electric field serves to create strained Si—O bonds. A complementary combination of field-induced polar-bond stretching and current-induced bond-catalysis seems to be required to explain quantitatively, at the molecular level, all the generally accepted TDDB observations.

Appendix A. Mie-Grüneisen bonding parameter η

$$\eta(m,n) = \left(\frac{mn}{m-n}\right)\left[\left(\frac{m+1}{n+1}\right)^{\frac{n+1}{n-m}} - \left(\frac{m+1}{n+1}\right)^{\frac{m+1}{n-m}}\right]$$

$n(m, n)$	$m = 12$	$m = 11$	$m = 10$	$m = 9$	$m = 8$	$m = 7$	$m = 6$
$n = 1$	0.66	0.64	0.62	0.60	0.58	0.55	0.52
$n = 2$	1.19	1.15	1.12	1.07	1.03	0.97	0.91
$n = 3$	1.64	1.59	1.53	1.47	1.39	1.31	1.22
$n = 4$	2.03	1.96	1.89	1.80	1.71	1.60	1.48
$n = 5$	2.38	2.29	2.20	2.09	1.98	1.85	1.70
$n = 6$	2.69	2.59	2.47	2.35	2.21	2.06	

References

[1] Anolick E, Nelson G. IEEE international reliability physics symposium (IRPS) proceedings, vol. 8; 1979.
[2] Crook D. IEEE-IRPS Proc 1979;1.
[3] Berman A. IEEE-IRPS Proc 1981;204.
[4] McPherson J, Baglee D. IEEE-IRPS Proc 1985;1.
[5] Swartz G. IEEE Trans On Elect Devs 1986;ED-33:1826.
[6] Boyko K, Gerlach D. IEEE-IRPS Proc 1989;1.
[7] Suehle J et al. IEEE-IRPS Proc 1994;120.
[8] Charparala P et al. IEEE-IRPS Proc 1996;61.
[9] Kimura M. IEEE-IRPS Proc 1997;190.
[10] Suehle J, Chaparala P. IEEE Trans Elect Dev 1997;801.
[11] McPherson J, Mogul H. J Appl Phys 1998;84:1513.
[12] Cheung K. Technical digest of papers international electron devices meeting, vol. 719; 1999.
[13] McPherson J et al. J Appl Phys 2000;88:5351.
[14] McPherson J. IEEE Trans Elect Dev 2003;50:1771.
[15] McPherson J. J Appl Phys 2004;95:8101.
[16] Pompl T et al. IEEE-IRPS Proc 2005;388.
[17] McPherson J. IEEE-IRPS Proc 2007;209.
[18] Dumin D. Oxide reliability: a summary Of silicon oxide wearout. Breakdown and reliability. World Scientific Publishing; 2002.
[19] Strong A et al. Reliability Wearout Mechanisms in Advanced CMOS Technologies. Series on microelectronic systems. IEEE Press; 2009.
[20] McPherson J. Reliability physics and engineering. Springer Publishing; 2010.
[21] Chen I, Hu C. IEEE-IRPS Proc 1985;24.
[22] Lee J, Hu C. IEEE-IRPS Proc 1988;131.
[23] Moazzami R, Hu C. IEEE Trans Elect Dev 1989;36:2462.
[24] Schuegraph K, Hu C. IEEE-IRPS Proc 1993;7.
[25] Hu C, Lu Q. IEEE-IRPS Proc 1999;47.
[26] Helms C, Poindexter E. Rep Prog Phys 1994;57:791.
[27] Pauling, Linus. In: The nature of the chemical bond. Cornell (NY): Cornel University Press; 1960. p. 83–91.
[28] Lide D. In: Hand book of chemistry and physics. CRC Press; 2000. p. 5–22.
[29] Ruffa A. Phys Rev Lett 1970;25:650.
[30] Capron N et al. J Chem Phys 2002;117:1843.
[31] Sulimov V et al. Phys Rev B 2002;66:024108.
[32] Martin-Samos L et al. Phys Rev B 2005;71:014116.
[33] Hamann D. Phys Rev B 2000;61:9899.
[34] Bongiorno A et al. Phys Rev B 2000;62:R16326.
[35] Conley Jr J et al. J Appl Phys 1994;76:2872.
[36] Lenahan P et al. IEEE-IRPS Proc 2001;150.
[37] Lenahan P. In: Fleetwood M et al., editors. Defects in microelectronic materials and devices. CRC Press; 2009.
[38] Degraeve R et al. IEEE Trans. Elect. Devs. 1998;45:904.
[39] Sune J, Jimenez D, Miranda E. J. High Speed Electr Syst 2001;11:789.
[40] Nicollian P. IEEE-IRPS Proc 1999;47.
[41] Stathis JD. Technical digest of papers international electron devices meeting, vol. 167; 1998.
[42] DiMaria D et al. J Appl Phys 1993;73:3367.
[43] DiMaria D, Stasiak J. J Appl Phys 1989;65:2342.
[44] Wu E et al. IEEE Trans Elect Dev 2002;49:2244.
[45] Wu E et al. IEEE-IRPS Proc 2002;60.
[46] Noguchi et al. IEEE-IRPS Proc 2003;287.
[47] Chen F et al. IEEE-IRPS Proc 2006;46.
[48] Suzumura N. IEEE-IRPS Proc 2006;484.
[49] Lloyd J. IEEE-IRPS Proc 2010;943.
[50] Tsu R et al. IEEE-IRPS Proc 2000;348.
[51] Eissa M et al. Advanced metallization conference proceedings, vol. 559. AMC; 2004.
[52] Ogawa E et al. IEEE-IRPS Proc 2003;166.
[53] Haase G et al. IEEE-IRPS Proc 2005;466.
[54] Maria D, Stathis J. J Appl Phys 2001;89:1183.
[55] Vogel E et al. J Appl Phys 2001;90:2338.
[56] Heh D et al. Appl Phys Letts 2003;82:3242.
[57] Higgins R, McPherson J. IEEE-IRPS Proc 2009;432.